JOURNAL OF VIROLOGY, Aug. 1988, p. 2686–2695
0022-538X/88/082686-10$02.00/0

Vol. 62, No. 8

# *cis*-Acting Intron Mutations That Affect the Efficiency of Avian Retroviral RNA Splicing: Implication for Mechanisms of Control

RICHARD A. KATZ, MOSHE KOTLER,† AND ANNA MARIE SKALKA*

*Institute for Cancer Research, Fox Chase Cancer Center, 7701 Burholme Avenue, Philadelphia, Pennsylvania 19111*

Received 10 February 1988/Accepted 21 April 1988

**The full-length retroviral RNA transcript serves as (i) mRNA for the *gag* and *pol* gene products, (ii) genomic RNA that is assembled into progeny virions, and (iii) a pre-mRNA for spliced subgenomic mRNAs. Therefore, a balance of spliced and unspliced RNA is required to generate the appropriate levels of protein and RNA products for virion production. We have introduced an insertion mutation near the avian sarcoma virus *env* splice acceptor site that results in a significant increase in splicing to form functional *env* mRNA. The mutant virus is replication defective, but phenotypic revertant viruses that have acquired second-site mutations near the splice acceptor site can be isolated readily. Detailed analysis of one of these viruses revealed that a single nucleotide change at −20 from the splice acceptor site, within the original mutagenic insert, was sufficient to restore viral growth and significantly decrease splicing efficiency compared with the original mutant and wild-type viruses. Thus, minor sequence alterations near the *env* splice acceptor site can produce major changes in the balance of spliced and unspliced RNAs. Our results suggest a mechanism of control in which splicing is modulated by *cis*-acting sequences at the *env* splice acceptor site. Furthermore, this retroviral system provides a powerful genetic method for selection and analysis of mutations that affect splicing control.**

All replication-competent retroviruses encode at least three essential genes. The *gag* gene codes for the structural proteins of the virion core and capsid, the *pol* gene encodes reverse transcriptase and integration function and the *env* gene encodes the glycoproteins located in the viral lipid envelope. The full-length avian sarcoma-leukosis virus transcript (ca. 7 to 9 kilobases) is capped and polyadenylated in the nucleus and transported to the cytoplasm where it is translated to produce the *gag* ($Pr76^{gag}$) and *pol* ($Pr180^{gag\text{-}pol}$) precursor polypeptides (32) (Fig. 1A). Full-length RNA must also serve as genomic RNA and is assembled into progeny virions at the cell membrane. In the nucleus, some full-length molecules also function as pre-mRNA which is alternatively spliced to form *env* and, for the sarcoma viruses, *src* subgenomic mRNAs that contain a common 5′ leader (L) RNA (Fig. 1A).

The avian sarcoma-leukosis virus RNA leader consists of a long noncoding segment (containing three short open reading frames) followed by a translation initiation codon at position 380 (position 1 is the cap site) corresponding to the N terminus of the $Pr76^{gag}$ precursor (28). A splice donor site at position 397 is used to fuse (in translational frame) the initiation codon and 5 additional codons in the 5′ leader with the main body of the *env* gene. Fusion with the *env* splice acceptor site at nucleotide position 5078 results in formation of the complete open reading frame for the $Pr95^{env}$ precursor (Fig. 1). Thus, the methionine (initiator) and the first five amino acids (encoded by nucleotides [nt] 380 to 397) of the $Pr76^{gag}$ and $Pr95^{env}$ precursor are common (6). The *src* splice acceptor site occurs within a short noncoding segment between the *env* and *src* genes, and *src* mRNA splicing also uses the donor site at position 397 (31) (Fig. 1). Thus, retroviruses use a strategy that is similar to other animal viruses; the downstream genes are expressed through spliced mRNAs by using a large, common precursor RNA.

It is apparent that a proper balance between spliced and unspliced retroviral RNA must be maintained; too little splicing could lead to a severe reduction in infectious particles due to diminished *env* mRNA levels. Excessive splicing would diminish the pool of genomic RNA and also limit core and capsid formation due to a reduced level of *gag* mRNA. Alternative splicing (*env* versus *src*) must also be controlled such that the appropriate amounts of these subgenomic mRNAs are formed (Fig. 1). Very little is known about the mechanisms of control involved in these steps.

In general, viral or cellular pre-mRNA splicing can proceed via several pathways which may or may not involve modulation of splice site selection (for reviews, see references 9, 21, 26, and 29). (i) All of the introns in the pre-mRNA can be constitutively removed. (ii) Alternative splice site selection (e.g., one donor and multiple acceptor sites) can be modulated in a temporal or tissue-specific manner. This results in the formation of different mRNAs that encode structurally distinct proteins through inclusion or exclusion of certain coding exons. The fact that different splice sites are used in different tissues suggests that *trans*-acting regulatory factors are involved in splicing regulation. A well-studied example is the troponin T gene (1). (iii) Pre-mRNAs can be alternatively spliced but without any obvious temporal or tissue-specific regulation; examples include certain adenovirus and simian virus 40 viral pre-mRNAs (as reviewed by Green [9]). In this case, a single large RNA precursor can give rise to multiple mRNAs that encode unique proteins and thus allows an economical strategy for gene expression. The relative abundance of each of the alternatively spliced RNA products could reflect intrinsic structural features of the pre-mRNA (*cis* control). These structural features may affect the efficiency by which the splice sites are recognized by the cellular splicing machinery.

In retroviruses, an additional level of control is observed; portions of the full-length RNA transcripts are preserved to function as genomic RNA and *gag-pol* mRNA, thus creating a balance between full-length and spliced subgenomic RNA

* Corresponding author.
† Permanent address: Department of Molecular Genetics, The Hebrew University, Hadassah Medical School, Jerusalem, Israel.

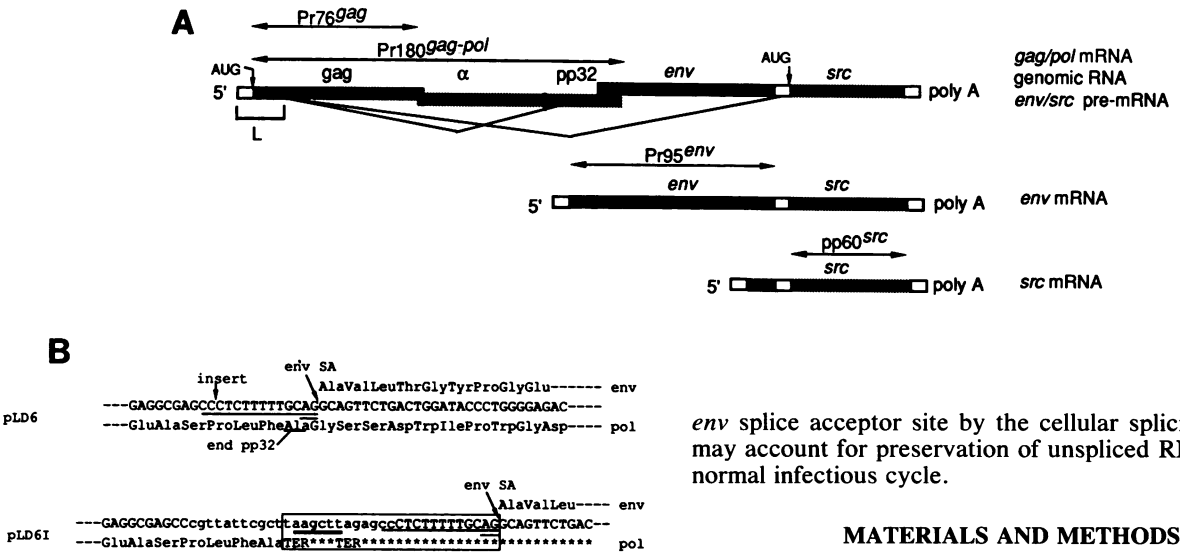


FIG. 1. (A) Structures of ASV genomic RNA, *gag-pol* mRNA, and *env* and *src* subgenomic mRNAs (not drawn to scale). The primary translation products are indicated above each mRNA. The AUG initiation codons for translation of the major products are indicated on the genomic RNA. □, Noncoding regions. The splice that forms the complete *env* reading frame for the *env* precursor ($Pr95^{env}$) is indicated. The AUG initiator and codons for the first five amino acids of $Pr95^{env}$ are provided by the mRNA leader (L). In the unspliced form of the RNA, this AUG serves to initiate translation of the $Pr76^{gag}$ and $Pr180^{gag\text{-}pol}$ precursors (6). Two of the *pol* gene products, the α subunit of reverse transcriptase and the pp32 endonuclease, are indicated. Overlapping reading frames between *gag-pol* and *pol-env* are indicated (not drawn to scale). Splice events that form *env* and *src* subgenomic mRNAs are indicated on the full-length transcript. ▬, Complete reading frame for the *env* precursor ($Pr95^{env}$). (B) Nucleotide sequence of wild-type (pLD6) and mutant (pLD6I) viral clones in the *env* splice acceptor site region. A *Ban*II restriction site (5'-GAGCCC-3', see arrow) located 12-nt upstream of the *env* splice acceptor site in pLD6 was used to introduce a 24-bp synthetic DNA fragment (nucleotides shown in lower case letters in pLD6I) via compatible sticky ends. The net affect of the insertion was to supply codons for the C terminus of the pp32 endonuclease and generate a 25-nt noncoding sequence between *pol* and *env* (boxed region). The splice acceptor site consensus sequence described by Mount (24) is underlined. The invariant AG dinucleotide comprising the 3' intron border is indicated by double underlining. *, Untranslated region that was generated by the mutation. SA, *env* splice acceptor site. The C-terminal amino acid of the mature pp32 endonuclease is indicated. A *Hin*dIII site present in the insert is marked with a bold line.

species (3). It is unclear whether maintenance of this balance requires virus-encoded *trans*-acting factors or results solely from the effects of *cis*-acting RNA sequences.

The studies presented here describe an avian sarcoma virus (ASV) mutant which is defective in splicing balance because of a mutation which was introduced near the splice acceptor site for *env* mRNA (Fig. 1). This mutant directs the synthesis of an abnormally high amount of accurately spliced, functional *env* mRNA. The mutant is replication defective, presumably because of a deficit of full-length RNA. We have exploited this ASV replication mutant as a genetic tool to isolate compensatory (suppressor) mutations which restore balanced splicing. Using this strategy, we have been able to identify sequences near the *env* splice acceptor site that influence the efficiency of splicing. From these results, we suggest that inefficient recognition of the *env* splice acceptor site by the cellular splicing machinery may account for preservation of unspliced RNA during the normal infectious cycle.

## MATERIALS AND METHODS

**Construction of ASV mutants containing altered splice acceptor regions.** The infectious ASV DNA clone, pLD6 (18), was used as substrate for mutagenesis. The pBR322-based pLD6 clone contains a complete, infectious, and transformation-competent DNA provirus of the Schmidt-Ruppin subgroup B strain of ASV. The pBR322 vector is inserted at a unique *Sal*I restriction site in the *env* gene. Infectious virus can be obtained by transfection of chicken embryo fibroblasts (CEFs) with *Sal*I-cleaved pLD6 DNA. Virus released from the transfected cells (ca. 1% of the total cells) can infect most of the remaining cells in the culture in about 6 days. At this time, the cells appear morphologically transformed because of expression of the viral *src* gene and viral particles can be detected by using a reverse transcriptase assay (see Fig. 2).

pLD6I was constructed as follows. A 259-base-pair (bp) *Kpn*I-*Xho*I fragment containing the *env* splice acceptor region (see Fig. 4B) was subcloned into the pBR322 derivative, pMG4 (14), by using standard methods (20). The resulting clone, pMG4-ENVB, contained a unique *Ban*II restriction site located 12 nt upstream of the *env* splice acceptor site (Fig. 1B). A synthetic 24-bp DNA fragment containing ends which are compatible with *Ban*II restriction sites was inserted. The insertion generated a 25-nt noncoding segment between the *pol* and *env* genes (Fig. 1B) and provided the last four codons for the pp32 *pol* protein. The two partially complementary oligonucleotides which composed the fragment were 5'-CGTTATTCGCTTAAGCTTA GAGCC-3' and 5'-CTAAGCTTAAGCGAATAACGGGCT-3'. The final mutant virus clone, pLD6I, was constructed by inserting the altered *Kpn*I-*Xho*I fragment containing the synthetic segment into pLD6. The nucleotide sequence of the altered *Kpn*I-*Xho*I fragment was confirmed by using the chemical sequencing method (22). As a control, the *Kpn*I-*Xho*I fragment from the wild-type pLD6 clone was used to reconstruct pLD6. The analogous *Kpn*I-*Xho*I fragment was isolated from a molecular clone of the revertant virus from culture 1 (see Fig. 4 and below). This fragment was substituted into pLD6 to generate pLD6IS-1.

**Transfection of avian cells.** The pLD6 viral clone and derivatives were cleaved with *Sal*I to release the pBR322 vector. The DNA was used to transfect CEFs by using the DEAE-dextran method as previously described (14). Media was harvested up to 4 weeks posttransfection and assayed for virus production by using the reverse transcriptase spot

assay (7). Under these conditions, virus can be detected only if multiple rounds of infection occur in the culture. QCl-3 cells were grown and transfected as previously described (14). The ability of the mutant viral clone to provide *env* in *trans* was tested by using a quantitative envelope complementation assay described previously (4). Briefly, Bryan high-titer Rous sarcoma virus (BH-ASV)-infected QCl-3 cells were transfected with pLD6I or pLD6 (wild-type) DNAs by using the DEAE-dextran method. The infectious BH-ASV transformation-competent viruses formed by complementation were assayed by using a standard focus assay on CEFs.

**Molecular cloning of a segment of a revertant viral genome.** Culture supernatants containing high titers of revertant viruses were collected and used to infect fresh cultures of CEFs in the presence of 5 μg of DEAE-dextran per ml. Cells were harvested at 22 to 44 h postinfection, and low-molecular-weight DNA was prepared by the method of Hirt (10). The DNA was treated with RNase and then digested with *Eco*RI. The DNA was ligated to *Eco*RI-digested pBR322 DNA which had been treated with calf intestinal phosphatase (Boehringer Mannheim). The DNA was then used to transform *Escherichia coli*, and the colonies were screened for appropriate viral sequences by using a probe derived from pLD6.

**S1 nuclease assay.** Mismatching of hybrids between viral genomic RNA and DNA probes was detected by using S1 nuclease (Boehringer Mannheim). Using the annealing and digestion conditions described previously (19), we were able to detect a single base mismatch. To screen for putative suppressor mutations near the *env* splice acceptor, the following method was used. Supernatant media (10 ml) were harvested from cultures of CEFs which were chronically infected with phenotypic revertant viruses. The supernatant media were centrifuged at 2,000 rpm in a Beckman TJ-6 centrifuge to remove cells. The resulting supernatant media were centrifuged at 30,000 rpm in a Beckman 70 Ti rotor for 1 h to pellet viral particles. The viral pellets were suspended in 200 μl of a solution containing 20 mM Tris hydrochloride (pH 7.4), 10 mM EDTA, 0.1% sodium dodecyl sulfate, 200 μg of proteinase K (EM Science) per ml, and 20 μg of *E. coli* tRNA. After incubation for 1 h at 37°C, the mixtures were extracted with phenol and ethanol precipitated. The RNAs were collected by centrifugation and suspended in 50 μl of water. From 5 to 10 μl was used for S1 nuclease protection assays. The DNA probes were prepared as follows. The *Kpn*I-*Xho*I *env* splice acceptor fragment was subcloned into the pBR322-derived pMG4 vector. pMG4 contains a synthetic segment that replaces the *Eco*RI-*Sph*I fragment of pBR322 and contains unique *Kpn*I and *Xho*I restriction sites. Three pMG4 derivatives were constructed, containing either the *Kpn*I-*Xho*I *env* splice acceptor fragment from the wild-type (pLD6), the mutant (pLD6I), or the revertant (pLD6IS-1). 5′-End-labeled probes complementary to the viral genome were produced by cleaving the pMG4 derivatives (containing the *Kpn*I-*Xho*I *env* splice acceptor fragment) at the *Xho*I site, followed by labeling with [$\gamma$-$^{32}$P]ATP by using polynucleotide kinase (Boehringer Mannheim). The probe fragment was produced by digestion with *Aat*II or *Ssp*I, both of which cleave in the pBR322 sequence just upstream of the *Kpn*I site. This strategy produced probes that contained ca. 50 to 75 nt of pBR322 sequences at the unlabeled end of the probe (see Fig. 4B). The pBR322 sequences allow the distinction between reannealed probe and probe which is protected by viral RNAs. A similar strategy was used to produce 5′-end-labeled probes complementary to the viral RNA genome. The pMG4 derivatives were cleaved with *Asp*718, which is an isoschizomer of *Kpn*I that generates 5′-protruding ends. This end was labeled by repair synthesis by using DNA polymerase I Klenow fragment. The probe fragment was produced by cleavage at the *Sal*I site in the pBR322 portion of the plasmid; this generated a probe containing pBR322 sequences at the unlabeled end. The probes were purified by preparative polyacrylamide gel electrophoresis.

The conditions for the S1 assay were as follows. The DNA probes were mixed with virion RNA samples and were ethanol precipitated in the presence of 20 μg of *E. coli* tRNA. The pellet was suspended in 2 μl of water, and 18 μl of the following solution was added: 90% formamide (Fluka), 0.5 M NaCl, 50 mM PIPES [piperazine-*N*,*N*′-bis(2-ethanesulfonic acid)] (pH 6.8), and 1 mM EDTA. The mixture was overlaid with oil, heated to 70°C for 10 min, and then incubated at 49°C for 16 to 20 h. The reaction mixtures were diluted to 200 μl with S1 nuclease buffer (0.25 M NaCl, 30 mM sodium acetate (pH 4.6), 1 mM $ZnSO_4$, 2 mg of denatured calf thymus DNA per ml) containing 200 U of S1 nuclease (Boehringer Mannheim). The reaction was incubated for 1 h at 37°C and stopped by adding EDTA to a concentration of 10 mM. After the addition of 20 μg of tRNA, the reaction mixture was extracted with water-saturated ether to remove the oil layer, phenol extracted, and ethanol precipitated. The pellet was suspended in formamide loading buffer, heated at 99°C for 2 min, and fractionated on a 7% polyacrylamide sequencing gel containing 7 M urea. Under these conditions, single base mismatches between DNA probes and viral RNA could be detected. For reasons that are unclear, mismatches were more readily detected in virion-derived RNAs than in the equivalent infected-cell RNA.

To measure the relative levels of spliced and unspliced RNAs in infected cells, the same methodology was used except that transfected or infected-cell RNA was used. The 5′-labeled probes were used as indicated below (see Fig. 3).

## RESULTS

**Construction of the *env* splice acceptor mutant.** The ASV *env* splice acceptor conforms to the consensus sequence described by Mount (24): $(T/C)_nN(T/C)AG \downarrow G$. In contrast to the situation for most cellular pre-mRNAs, this *cis*-acting sequence (CCCTCTTTTTGCAG ↓ G) also encodes a *trans* function: codons for the C terminus of the mature viral *pol*-endonuclease gene product, pp32 (Fig. 1). The GCA codon in the splice consensus sequence encodes the C-terminal amino acid of the mature pp32 *pol* product (8). The remaining C-terminal 37 amino acids of the primary *pol* translation product ($Pr180^{gag\text{-}pol}$) are removed by proteolytic processing and are dispensable for replication (13). We had designed an insertion mutation (described in detail below) to address the functional role of this C-terminal *pol* fragment. The mutation (Fig. 1B) created a 25-nt noncoding segment between the *pol* and *env* genes which normally overlap over a distance of ca. 100 nt (28). In this mutant, pLD6I, the splice acceptor consensus sequence and neighboring 5′ sequences are no longer required for *pol* coding. Therefore, this mutant genome provides a system by which further mutations can be introduced at the *env* splice acceptor site without affecting *pol* functions. Since the products of both the spliced and unspliced forms of the viral transcript are required for replication, the effects of mutations can be readily monitored by using viral growth and genetic complementation assays.

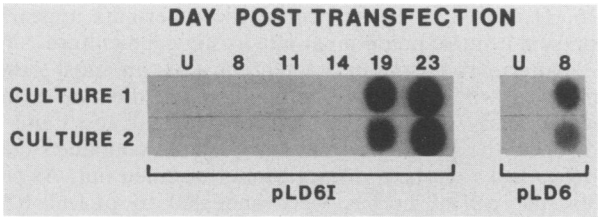


FIG. 2. Reverse transcriptase assay of transfected-CEF culture supernatants. Parallel CEF cultures (cultures 1 and 2) were transfected with the wild-type (pLD6) or the mutant (pLD6I) viral clones. On the indicated days, a reverse transcriptase assay was performed on the culture supernatants. The $^{32}$P-labeled DNA products were spotted onto DEAE paper as previously described (7), and the paper was exposed to X-ray film.

The mutation consists of a 24-bp synthetic DNA fragment which was inserted into a *Ban*II restriction site (5'-GAGCCC-3') located at the 5' end of the pyrimidine stretch of the splice acceptor consensus sequence (−12 from the splice acceptor site; Fig. 1B). The 5' 11 bp of the insert provide four codons for the mature C terminus of the pp32 product which is normally encoded by the splice acceptor consensus nucleotides. However, to prevent loss via recombination, the introduced codons were altered by first and third position changes such that nucleotide sequence homology to the splice acceptor consensus sequence was destroyed. The 3' 13 bp of the insert encode two in-frame *pol* termination codons and a *Hin*dIII restriction site (5'-AAGCTT-3') for identification of clones containing the insert. The effect of the mutation was to separate the known *cis* and *trans* functions in this region. The *cis*-acting *env* splice acceptor site was retained in its original form, while the *pol*-coding function was provided by the insert.

**Genetic analysis of the splice acceptor site insertion mutant.** Transfection of CEFs with the mutant viral DNA (pLD6I) did not result in efficient virus spread. Virion-associated reverse transcriptase activity could not be detected in supernatants from two parallel cultures up to 14 days posttransfection (Fig. 2); such activity was readily detected by 8 days after transfection with wild-type parent virus (pLD6). However, after long-term passage (19 days) of mutant-transfected cells, replication-competent viruses were detected in culture supernatants (Fig. 2). Since ASV is able to transform CEFs via the *src* gene product, we could also visually monitor the culture for the production and spread of these late-appearing viruses. The origin of these viruses will be discussed below.

The nature of the defect in pLD6I was examined by using a genetic assay. We have shown previously, using one of the late-appearing viruses to be described below, that the *pol* reading frame truncation in pLD6I does not detectably affect ASV replication (13). Therefore, the defect in pLD6I appeared to be acting in *cis* and could possibly affect some aspect of RNA splicing because of the proximity of the mutation to the *env* splice acceptor site. We tested whether the pLD6I mutant could provide *env* function in *trans* by using a quantitative genetic complementation assay (4). The assay is based on the ability of *env* gene products synthesized from a transfected DNA clone to complement an ASV envelope-deleted, transformation-competent mutant, BH-ASV, in a chronically infected quail cell line (QCl-3). The results showed that pLD6I was able to complement BH-ASV as efficiently as the wild type (pLD6) or a reconstructed wild-type genome (pLD6R) (Table 1). Thus, pLD6I is not impaired in the ability to synthesize and translate *env* mRNA.

TABLE 1. Analysis of pLD6I growth and *env* protein production by transfection of avian cells[a]

| Viral genotype | Clone designation | Growth on CEFs | *env* complementation activity relative to pLD6 (wild type)[b] |
|---|---|---|---|
| Wild type | pLD6 | + | 1.0 |
| Reconstructed wild type | pLD6R | + | 1.7 |
| Mutant | pLD6I | − | 2.6 |

[a] Viral DNA clones were tested for their ability to produce infectious virus after transfection of CEFs or to provide the *env* gene product in *trans*. The wild-type clone (pLD6) was compared with a reconstructed wild-type clone (pLD6R) and the insertion mutant (pLD6I). pLD6R was reconstructed by using a *KpnI-XhoI* fragment containing the *env* splice acceptor site from wild-type virus. *env* complementation experiments were performed by transfection of QCl-3 cells that are chronically infected with an *env*-deleted virus (BH-ASV) as previously described (4).

[b] Complementation was measured by using a viral focus assay; the number of foci produced are expressed relative to the pLD6 (wild-type) clone. In this experiment, approximately 100 to 200 focus-forming units were released per dish of transfected QCl-3 cells.

**Analysis of *env* mRNA in wild-type and mutant-transfected cells.** To further evaluate pLD6I mRNA production, we performed S1 nuclease protection assays. BH-ASV-infected QCl-3 quail cells were again used as a recipient for transfection with cloned wild-type (pLD6) and mutant (pLD6I) viral DNAs. The viral DNAs were introduced by using the DEAE-dextran-mediated transfection method, and *env*-containing transcripts were analyzed at 60 h posttransfection. At this early time, all of the viral RNA is synthesized from the transfected DNA template rather than in newly infected cells (14). Since quail cells are resistant to subgroup B virus, little, if any, mRNA is expected to be produced through infection. The probes used for S1 analysis of *env* mRNA and unspliced RNA spanned the *env* splice acceptor region. In both cases, the probes were entirely homologous to the viral clone. A positive control (Fig. 3, lane 6) shows that the pLD6I-derived probe was protected by virus-specific RNA containing the homologous mutant sequence synthesized in *E. coli*. As expected, because of the BH-ASV *env* deletion, no *env* mRNA was detected in mock-transfected, BH-ASV-infected QCl-3 cells (lanes 1 and 2). In pLD6 (wild-type)-transfected cells, the ratio of unspliced RNA to *env* mRNA was approximately 2:1 (lane 3). A similar ratio was seen in CEFs chronically infected with pLD6 virus (lane 5). In pLD6I-transfected cells, the wild-type splice acceptor site for *env* mRNA appears to be used (lane 4). The level, however, was significantly higher, and the ratio of unspliced RNA to *env* mRNA was approximately 1:5 (lane 4). We conclude from these results that the insert near the *env* splice acceptor site causes an increase in the steady-state level of *env* mRNA and a concomitant decrease in the level of unspliced RNA. This observation is consistent with the genetic complementation described above and indicates that more efficient, accurate splicing at the *env* splice acceptor site occurs in the pLD6I mutant.

**Isolation and characterization of phenotypic revertants of the pLD6I mutant.** As noted above, after prolonged passage of pLD6I-transfected cells, infectious viruses were detected in the culture media (cf. Fig. 2). These viruses could have arisen from (i) slow growth of the mutant virus; (ii) reversion (deletion) of the pLD6I mutation, giving rise to the wild-type virus; or (iii) second-site suppressor-type mutations which restore splicing control and, thus, relieve the replication defect. To rapidly discriminate between these possibilities, we used an S1 nuclease-based mismatch detection assay.

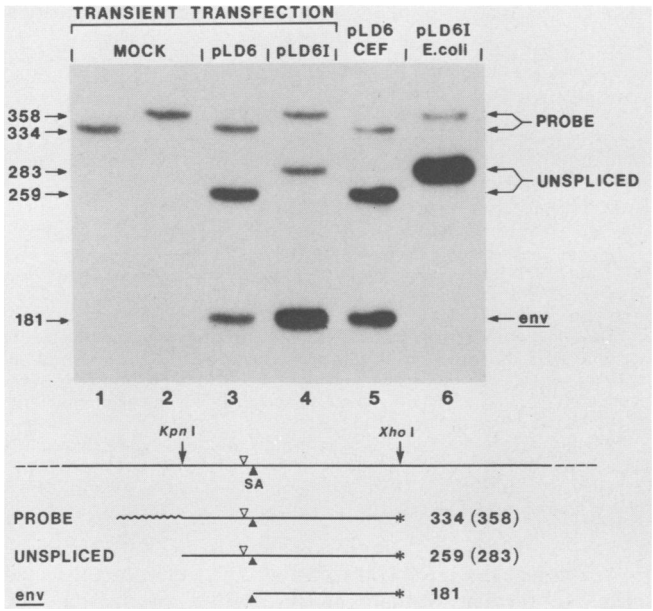


FIG. 3. S1 nuclease protection assay for measuring the ratio of *env* mRNA to unspliced RNA in transfected or infected cells. Protected DNA fragments from the S1 nuclease assay were fractionated on a 7% acrylamide-urea gel. The end-labeled probe was synthesized as described in Materials and Methods. The probe was constructed by cleaving pMG4-ENVB with *Xho*I and end labeling with [$\gamma$-$^{32}$P]ATP by using T4 polynucleotide kinase. A second cleavage in the pBR322 portion of the clone resulted in generation of a probe containing pBR322 sequences at one end (~~~). Two probes were synthesized: one derived from pLD6 and one derived from pLD6I (see map below). ▽, Position of the mutagenic insert in pLD6I; ▲, splice acceptor site (SA). Lengths of fragments are indicated in nucleotides. Numbers in parentheses indicate lengths of fragments which include the pLD6I-derived mutagenic insert. The sources of the cellular RNAs used in protection experiments are indicated. Lanes 1 to 4, QCl-3 cells transiently transfected with the indicated clones and harvested 60 h posttransfection. RNAs from these cultures were assayed with the homologous S1 probe: pLD6 with a 334-nt probe and pLD6I with a 358-nt probe. As a negative control, RNAs from a mock-transfected culture were assayed with both probes; lane 1, 334-nt probe; lane 2, 358-nt probe. Lane 5, RNA from pLD6-infected CEF cells. A control RNA, which is homologous to the viral portion of the 358-nt probe, was synthesized in *E. coli* under control of the lambda bacteriophage $p_L$ promoter (lane 6).

RNA was prepared from virions isolated on day 19 or day 27 posttransfection and was annealed to end-labeled pLD6I splice acceptor fragment probes (Fig. 4). For each of two independent viral isolates obtained from the separately transfected cultures described in the legend to Fig. 2, S1 nuclease cleaved mismatched regions within the 283-nt splice acceptor segment tested (Fig. 4A and 4B). In the isolate from culture 1, the mismatched region mapped within the 24-nt insert (the original mutation) and appeared to result from a minor change since the hybrid was only partially cleaved by S1 nuclease at this site (lanes 3, 4, 9, and 10). The change occurred very close to the introduced *Hin*dIII site in the insert, as indicated by comigration with probes that were digested with *Hin*dIII (lanes 2–4, 9, and 10). The mismatch mapped to the same position when a probe fragment labeled at the 5′ or 3′ ends was used (Fig. 4B). The isolate from culture 2 also contained an alteration which caused mismatching with the probe. However, this alteration occurred downstream of the *env* splice acceptor site and did not map to the same position with probes labeled at either end (lanes 5, 6, 11, and 12). These phenotypic revertants appear to represent a single predominating virus in each culture, since the pattern of mismatch protection was, in most cases, consistent with a unique mutation and it did not change between early and late viral harvests (e.g., lanes 3 and 4). However, the possibility that the cultures contained other independent revertant viruses cannot be ruled out. As controls, the pLD6I probes were annealed to pLD6I RNA synthesized in *E. coli* (lanes 7 and 13) and to wild-type viral RNA (lane 14). After annealing with wild-type viral RNA, the 3′-labeled probe was cleaved by S1 at a site corresponding to the 5′ border of the insert, as expected. From these results, we conclude that the late-appearing viruses contain mutations near the *env* splice acceptor site.

**A phenotypic revertant virus encodes a suppressor-type mutation near the *env* splice acceptor site.** A 2.5-kbp *Eco*RI restriction fragment containing the *env* splice acceptor site was molecularly cloned from the unintegrated form of viral DNA isolated after infection of CEFs with the virus from culture 1 (Fig. 2). Nucleotide sequence analysis of the 283-bp *Kpn*I-*Xho*I fragment which spans the *env* splice acceptor site revealed a single nucleotide difference (T to C) from pLD6I within the original 24-nt insert (Fig. 5). The change destroyed the *Hin*dIII site present in the insert. This change maps to the position identified by the S1 nuclease mismatch assay of virion RNA (Fig. 4). Therefore, the viral DNA fragment, which was cloned and sequenced, is likely representative of the major viral RNA genome species identified in the culture supernatants.

To determine whether the nucleotide change was responsible for the phenotypic reversion of the pLD6I mutation, the 283-bp *Kpn*I-*Xho*I splice acceptor fragment, from the culture 1 viral DNA, was substituted into the wild-type clone (pLD6) to generate pLD6IS-1. CEFs were transfected in parallel with pLD6 (wild-type), pLD6I (mutant), and pLD6IS-1; pLD6I and pLD6IS-1 are isogenic except for the single nucleotide difference. The appearance of virus in the supernatant was measured by using a reverse transcriptase assay. pLD6IS-1 replicated like the wild type (Fig. 6). At a later time posttransfection (day 17), pLD6I gave rise to phenotypic revertant virus as observed previously (Fig. 2). From these results, we conclude that the single nucleotide difference between pLD61 and pLD6IS-1 can account for the phenotypic reversion.

**The phenotypic reversion in pLD6IS-1 results from a suppressor-type mutation which affects splicing efficiency at the *env* splice acceptor site.** The effect of the suppressor mutation in pLD6IS-1 on splicing was tested in a transient transfection assay. Cloned DNA of the wild-type (pLD6), mutant (pLD6I), and phenotypic revertant-derived (pLD6IS-1) virus was used to transfect QCl-3 cells, and the relative amounts of unspliced and *env* mRNA were measured by using the S1 protection assay. Probes that were homologous to the respective viral sequences were used in each case. The suppressor mutation in pLD6IS-1 had a significant effect on the relative levels of *env* mRNA and unspliced RNA (Fig. 7). Quantitation of the results is shown in Table 2. Consistent with previous experiments, the *env* mRNA/unspliced-RNA ratio in pLD6I-transfected cells was approximately 10-fold greater than in the wild type (pLD6) (Fig. 7, lanes 3 and 4). In contrast, in pLD6IS-1-transfected cells, the ratio was reduced by approximately fivefold compared with the wild type (Table 2). Thus, the suppressor mutation establishes a new steady-state ratio which is not identical to the wild type but is apparently adequate to support viral replication. CEFs which were chronically infected with pLD6IS-1 virus

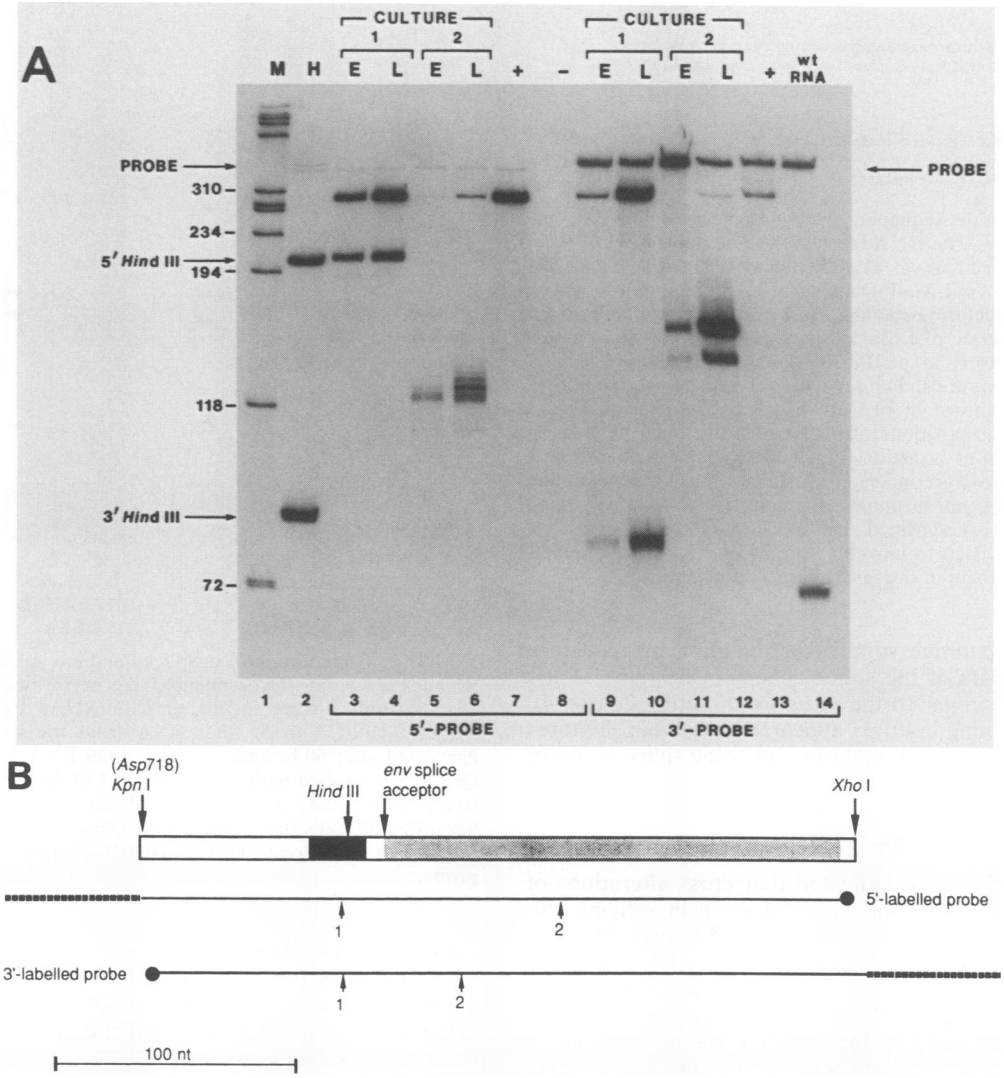


FIG. 4. Use of S1 nuclease mismatch detection assay to map putative suppressor mutations near the *env* splice acceptor site. (A) RNA was prepared from virus particles which appeared after transfection of CEFs with pLD6I (Fig. 2). RNA used for the S1 mismatch assay was prepared from early harvest (day 19) (lanes marked E) or late harvest (day 27) (lanes marked L) of virus. Cultures 1 and 2 correspond to those in Fig. 2. Protected end-labeled DNA fragments were fractionated on a 7.5% polyacrylamide sequencing gel containing urea. Probes were end labeled (●) by repair of an *Asp* 718 site (3′-labeled probe) or kinase labeling of the *Xho*I site (5′-labeled probe) (panel B). As markers, a mixture of the two probes was digested with *Hin*dIII (lane 2). Controls were as follows: lane 7, RNA synthesized in *E. coli* that is homologous to the viral portion of the pLD6I probe fragment; lane 8, no RNA; lane 14, wild-type RNA (pLD6). (B) Map of *env* splice acceptor site fragment and DNA probes used to detect mismatching. Probe strategy is indicated below the map. Presence of pBR322 sequences (▬ ▬ ▬ ▬) allows distinction between reannealed probe and probe completely protected by viral RNA sequences. Arrows (corresponding to viral RNA from cultures 1 and 2) indicate mismatch sites as detected by 3′- and 5′-labeled probes. ▭, *env* leader peptide-coding region (28).

showed a similar new steady-state level (Fig. 7, lanes 6 and 7; Table 2). Therefore, the phenotype is stable through multiple rounds of viral infection. A comparison of the absolute *env* mRNA levels among transfected cultures is difficult because different probes were used to detect viral RNA in mutant and wild-type transfected cells (Fig. 7). However, in several experiments, we have observed that the amounts of total viral RNA are nearly equivalent in cells transfected with the various viral clones (Fig. 7). Therefore, we conclude that the mutations described here affect the efficiency of splicing per se and that the absolute levels of *env* mRNA are most likely altered.

**The revertant phenotype is often associated with alterations near the acceptor splice site.** We used the S1 nuclease mismatch detection method to assay for nucleotide changes near the splice acceptor site in additional revertant viruses that appeared after transfection with the pLD6I mutant DNA (Fig. 8). Ten independent CEF cultures were transfected and passaged for 2 to 3 weeks, at which time phenotypic revertant viruses were detected by reverse transcriptase activity. Seven of the transfected cultures (corresponding to lanes 1, 2, 4, 5, 6, 7, and 10) gave rise to what appeared to be predominately single, revertant viruses as indicated by unique mismatch regions near the splice acceptor site. Probes labeled at either the 3′ or 5′ ends were used (data not shown for 3′-labeled probe). Most of these putative suppressor mutations mapped to a position near the introduced *Hin*dIII site (Fig. 5), but all did not map to precisely the same

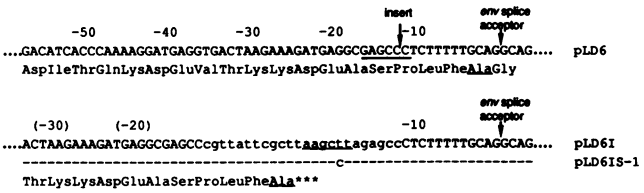


FIG. 5. Nucleotide sequence of revertant virus near the *env* splice acceptor site. The DNA form of the revertant provirus from culture 1 was cloned as an *Eco*RI fragment, and the nucleotide sequence of the *Kpn*I-*Xho*I fragment containing the *env* splice acceptor site was determined. The *Kpn*I-*Xho*I fragment was cloned into pLD6 to generate pLD6IS-1. Shown are the relevant regions. The mutagenic insert in pLD6I is shown in lowercase letters. Nucleotide positions are shown relative to the splice acceptor site in pLD6. Positions shown in pLD6I and pLD6IS-1 in parentheses indicate the shift in positions of nucleotides upstream of position −12 due to the 24-nt insertion. Nucleotides that are identical in pLD6I and pLD6IS-1 are indicated by dashes. Deduced *pol* amino acids are shown. *, *pol* termination codon. The C-terminal amino acid of pp32 (*Ala*) is underlined. The *Ban*II (5′-GAGCCC-3′) site in pLD6, which was used to introduce the 24-bp fragment, is underlined. The *Hin*dIII site in the insert in pLD6I is underlined.

positions. One putative suppressor mutation mapped to a region downstream of the splice acceptor site (lane 5) and appeared to be similar to the virus from culture 2 (Fig. 4). The three remaining cultures appeared to contain mixtures of viruses all of which had mutations near the splice acceptor site.

## DISCUSSION

Previous studies have indicated that gross alterations of retroviral introns can result in a reduction in splicing efficiency (11, 23) or activation of cryptic splice sites (25). Our studies are based on a novel ASV mutant, pLD6I, which was produced by in vitro mutagenesis. The mutation consists of a 24-nt insertion located 12-nt upstream of the *env* splice acceptor. The net affect of the insertion was to introduce a 25-nt noncoding region between the *pol* and *env* reading frames which normally overlap over a span of ca. 100 nt (Fig. 1). This eliminated the reading frame for a 37-amino-acid C-terminal *pol* fragment which is normally proteolytically removed during maturation of the pp32 *pol* product and is not required for replication (13). More importantly, the

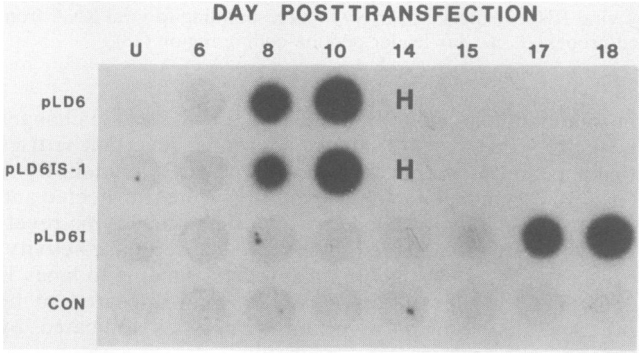


FIG. 6. Reverse transcriptase assay of transfected CEF culture supernatant. CEF cultures were transfected with the indicated viral constructs and assayed for reverse transcriptase activity on various days posttransfection as described for Fig. 2. The pLD6 and pLD6IS-1 cell cultures were harvested after day 10 (H).

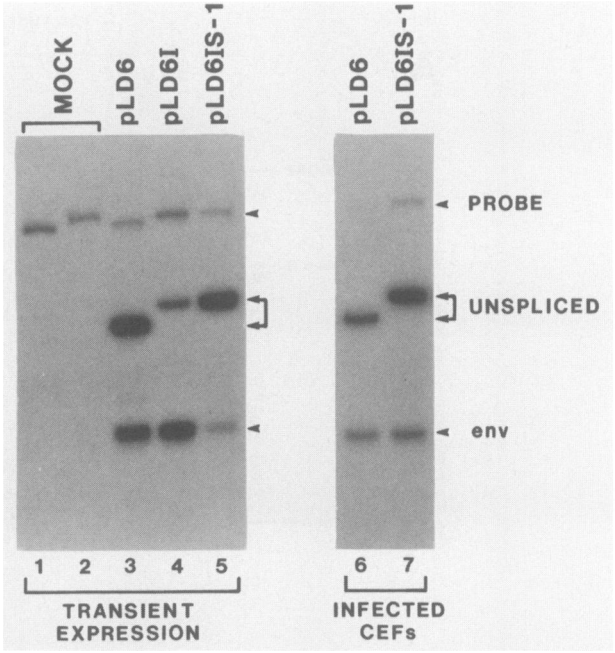


FIG. 7. Quantitation of unspliced and *env* mRNA transcripts by S1 nuclease assay. Experiments were performed as described for Fig. 3. Probes were incubated with RNAs from the following sources: lanes 1 to 5, total RNA from transfected QCl-3 cells harvested after 60 h; lanes 1 and 2, total RNA from untransfected QCl-3 cells probed with pLD6 and pLD6I-derived probes, respectively; lanes 6 and 7, total RNA was from chronically infected CEFs harvested 10 days posttransfection. Designations above lanes correspond to viral clones used for transfection and corresponding S1 probe.

resulting noncoding segment which was created between the genes includes the 3′ border of the *env* intron (Fig. 1B). Thus, in this construct, a region which may be involved in splicing control can readily accept mutations without affecting *pol* coding functions.

The pLD6I mutant has an unusual phenotype; it is replication defective but can provide *env* in *trans* in a genetic complementation assay (Table 1). Since the initiation codon for the *env* precursor ($Pr95^{env}$) is provided through the splicing event (Fig. 1), these results suggest that *env* mRNA

TABLE 2. Ratio of *env* mRNA to unspliced RNA levels in cells transfected with wild-type, mutant, and revertant viral DNA clones

| Viral clone | Phenotype | Expression[a] | *env* mRNA/unspliced-RNA ratio[b] | |
|---|---|---|---|---|
| | | | Expt 1 | Expt 2 |
| pLD6I | Mutant | Transient | 6.30 | 4.40 |
| pLD6 | Wild type | Transient | 0.53 | 0.48 |
| pLD6IS-1 | Revertant | Transient | 0.10 | 0.13 |
| pLD6 | Wild type | Chronic | 0.54 | 0.44 |
| pLD6IS-1 | Revertant | Chronic | 0.23 | 0.29 |

[a] Transient, Total RNA was harvested 60 h posttransfection of QCl-3 cells; chronic, CEF cells were transfected with the indicated infectious DNA clones and the total cellular RNA was harvested after multiple rounds of infection had occurred (ca. 10 days).

[b] Autoradiographs of S1 analyses similar to Fig. 7 were scanned with a laser densitometer. The ratios of peak areas are indicated. Experiments 1 and 2 represent individual S1 assays performed on the same RNA samples.

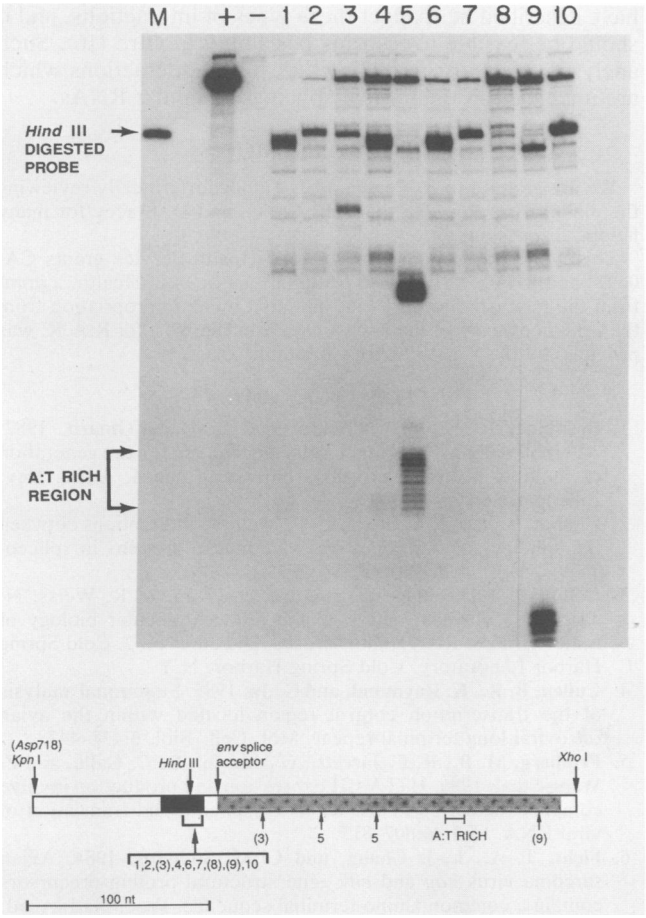


FIG. 8. S1 nuclease mismatch detection assay of independent revertants. Ten CEF cultures were transfected with pLD6I and passaged for 2 to 3 weeks, at which time phenotypic revertant viruses were identified in each culture. Virion RNA from the revertants was assayed by using the 5′ probe indicated in Fig. 4B. The 5′-labeled pLD6I-derived probe was cleaved with *Hin*dIII (Fig. 4B) to serve as a marker corresponding to the region ca. −20 from the *env* splice acceptor site (lane M). Lanes 1 to 10 correspond to cultures 1 to 10, respectively. Minor bands in lanes 1 to 10 likely correspond to A+T-rich regions which become sensitive to S1 when neighboring mismatches occur. A major A+T-rich region (18/20) is indicated. Controls were RNA synthesized in *E. coli* that corresponds to the viral segment of the pLD6I probe (+) and probe incubated with no RNA (−). The map below indicates mismatch sites (arrows) detected by using 3′- and 5′-labeled probes. Numbers below arrows correspond to individual cultures from which the revertant viral RNA was derived. Numbers in parentheses indicate that these cultures appeared to contain a mixture of revertant viruses or showed an ambiguous pattern when 3′ and 5′ probes were compared. Mismatched sites were mapped by using 3′- and 5′-labeled probes which were cleaved with several restriction enzymes and electrophoresed in parallel as markers (not shown). Stippled area indicates *env* leader peptide-coding region.

is formed properly. RNA studies indicated that the pLD6I *env* mRNA was accurately spliced but the *env* mRNA/unspliced-RNA ratio was 10-fold higher in mutant-transfected cells, apparently because of an increase in the efficiency of splicing (Table 2). These analyses were carried out in cells (QCl-3) that provide *gag*, *pol*, and *src* products in *trans* through expression of *env*-deleted BH-ASV. Since BH-ASV proteins were not able to complement the pLD6I splicing defect at the RNA level (Fig. 3), we conclude that the mutation acts in *cis*. The *cis*-acting nature of the defect was predicted since the insertion mutation does not affect any *pol* coding region known to be required for replication (13).

We reasoned that if the replication defect was due to an imbalance in the levels of full-length RNA versus *env* mRNA, phenotypic reversion would require restoration of control and that analysis of such mutants would identify splicing control regions. After prolonged passage of pLD6I-transfected CEFs, replication-competent, phenotypic revertant viruses arose which contained second-site mutations near the *env* splice acceptor site. Mapping the second-site mutations on the viral genomic RNA derived from early and late harvests suggested that single revertant viruses predominated in each of the two cultures (Fig. 4). Further molecular cloning, sequencing, and genetic and S1 analyses of RNA species in transfected cells indicated that a single nucleotide change at position −20 from the *env* splice acceptor in one revertant was sufficient to restore viral growth and also resulted in preservation of unspliced RNA. Remarkably, the unspliced form was preserved in an overcompensating way and resulted in a ca. two- to fivefold reduction in the *env* mRNA/unspliced-RNA ratio as compared to the wild type (Table 2). Although we have not completed the analysis of other revertant viruses (Fig. 8), we expect that these changes also increase the level of unspliced RNA. Taken together, these data indicate that the original insertion mutation in pLD6I created a better splice acceptor site and that this resulted in a deficit of full-length RNA. An alternative explanation, such as RNA instability due to the insertion, seems unlikely for two reasons. First, the total amount of viral RNA in transfected cultures appeared to be constant (Fig. 3 and 7). Second, the mutagenic insert remains unaltered in at least one of the revertants (Fig. 4); thus, its presence, per se, does not account for the defect.

This system imposes two limits on selection for revertants. First, it selects for viral growth and, thus, regulated splicing. Second, it provides a bias in selection for suppressor mutations at the splice acceptor site by providing a noncoding segment which can readily accept changes. It seems possible that the system could also select for (i) mutations in a putative viral protein which controls splicing or (ii) some other *cis*-acting mutations that fall in essential coding regions. These two classes of mutations would be predicted to occur with lower frequency. In this regard, two independent revertants (Fig. 4, culture 2; Fig. 8, culture 5) have acquired second-site mutations downstream of the *env* splice acceptor site, within the *env* leader peptide-coding region. In both cases, the second-site mutation maps to two positions ca. 30-nt apart, indicative of a large deletion or a double mutation within the *env* leader region (cf. maps in Fig. 4 and 8). However, the 62-amino-acid *env* leader peptide is an unlikely candidate for a splicing regulatory protein since it is involved in membrane insertion of the *env* precursor protein and is removed by the cellular signal peptidase (33). It seems more likely that these second-site mutations also act in *cis* to affect splicing. The effect of these changes may be tolerated with respect to the coding capacity of the *env* leader peptide; its role in membrane insertion may not be significantly affected.

As indicated in Fig. 1A, the expression of *env* and *src* mRNAs depends on an alternative splicing strategy. In the experiments presented here, we have not directly addressed the effect of *env* splicing mutations on *src* mRNA splicing. However, all of the revertant viruses that we have identified (Fig. 4 and 8) express sufficient levels of *src* to cause cell transformation. Most probably, *src* expression is not af-

fected in pLD6I; excessive *env* splicing may not preclude *src* mRNA splicing. However, as noted by others (31), ASV *src* mRNA splicing efficiency can also be affected by minor nucleotide changes near the splice acceptor site.

How do the spontaneous revertants of pLD6I arise? They could arise by misincorporation of nucleotides during RNA polymerase II transcription of proviral DNA or in infected cells during reverse transcription. Either mechanism requires that some unspliced RNA in pLD6I-transfected cells reaches the cytoplasm to serve as viral genomic RNA and *gag-pol* mRNA. Although there is a deficit of unspliced RNA, it can be detected readily and represents ca. 10% of the *env* mRNA in transiently transfected cells (Fig. 3 and 7). Therefore, pLD6I probably gives rise to a partially defective virus. It may spread slowly within the cultures, below levels that can be detected by using the reverse transcriptase assay. Once a revertant virus arises, it is able to spread rapidly and become the major viral species in the culture.

Several possible mechanisms could account for the balance of unspliced and spliced retroviral RNAs (as noted by Coffin [3]). (i) A viral-encoded protein could be involved in "protecting" a portion of RNA from splicing, resulting in the preservation of some full-length RNA as may be the case in two human viruses, human T-cell leukemia virus type I (12) and human immunodeficiency virus type 1 (5). (ii) Some full-length RNA could be rapidly or selectively transported to the cytoplasm, thus evading the nuclear splicing machinery; this could also be mediated by a virus-encoded protein. (iii) The splice site could be poorly recognized by the cellular splicing machinery because of a primary or secondary structural feature of the RNA molecule. Although mechanisms i and ii are not excluded, our results show that the splicing balance can be disrupted and reinstated by *cis*-acting changes in sequences at the acceptor site. Thus, the simplest interpretation of our data would support the third mechanism. The fact that genetic selection for viral growth resulted in the acquisition of *cis*-acting suppressor mutations at the *env* splice acceptor site suggests that regulated (inefficient) splicing may have been selected for in a similar manner during evolution of these viruses.

What is the nature of this *cis*-acting control? It seems unlikely that the insertion mutation destroyed a specific recognition sequence for a virus-encoded control protein since the suppressor mutation in pLD6IS-1 (a T-to-C change) occurred within the mutagenic insert. However, the nucleotide change in pLD6IS-1 does not destroy or create any known splicing consensus sequence including a chicken lariat target site consensus sequence (CTPuAPy) (15), a cryptic 3′ intron border (AG ↓ G), or the splice acceptor consensus sequence [$(Py)_nXPyAG \downarrow G$]) (24). Perhaps the insertion in pLD6I removes an RNA structural restraint to recognition of the splice acceptor and the suppressors reimpose the restraint. RNA secondary structure has been shown to affect the efficiency of splicing (30).

The initial interaction of the pre-mRNA with the cellular splicing machinery is thought to occur at the splice acceptor site. For example, studies with globin pre-mRNA have shown that a sequence immediately upstream of the 3′ splice acceptor, including the pyrimidine stretch and the lariat target site, is protected by the U2 small nuclear ribonucleoprotein particle in mammalian cell extracts (2) and that this interaction may commit the RNA to splicing (17). Furthermore, recent genetic evidence has indicated that the U2-like small nuclear ribonucleoprotein particle RNA of yeast is involved in Watson-Crick base pairing with the lariat target sequence (27). It seems possible that the mutations that we have described here affect these types of interactions, and it should be feasible to test this possibility in vitro (16). Such analyses could also provide clues to the interactions which are important in the normal splicing of cellular RNAs.

## ACKNOWLEDGMENTS

We are grateful to R. Perry and J. Taylor for critically reviewing the manuscript. We also thank B. Cullen and D. Stacey for many helpful discussions.

This work was supported by Public Health Service grants CA-06927 and RR-05539 from the National Institutes of Health, a grant from the Pew Charitable Trust, and also by an appropriation from the Commonwealth of Pennsylvania. Partial support for R.A.K. was provided by the W. W. Smith Charitable Trust.

## LITERATURE CITED

1. **Breitbart, R. E., A Andreadis, and B. Nadal-Ginard.** 1987. Alternative splicing: a ubiquitous mechanism for the generation of multiple protein isoforms from single genes. Annu. Rev. Biochem. **56**:467–495.
2. **Chabot, B., and J. A. Steitz.** 1987. Multiple interactions between the splicing substrate and small ribonucleoproteins in spliceosomes. Mol. Cell. Biol. **7**:281–293.
3. **Coffin, J.** 1985. Genome structure, p. 17–73. *In* R. Weiss, N. Teich, H. Varmus, and J. Coffin (ed.), Molecular biology of tumor viruses: RNA tumor viruses, 2nd ed., vol. 2. Cold Spring Harbor Laboratory, Cold Spring Harbor, N.Y.
4. **Cullen, B. R., K. Raymond, and G. Ju.** 1985. Functional analysis of the transcription control region located within the avian retroviral long terminal repeat. Mol. Cell. Biol. **5**:438–447.
5. **Feinberg, M. B., R. F. Jarrett, A. Aldovini, R. C. Gallo, and F. Wong-Staal.** 1986. HTLV-III expression and production involve complex regulation at the levels of splicing and translation of viral RNA. Cell **46**:807–817.
6. **Ficht, T. A., L.-J. Chang, and C. M. Stoltzfus.** 1984. Avian sarcoma virus *gag* and *env* gene structural protein precursors contain a common amino-terminal sequence. Proc. Natl. Acad. Sci. USA **81**:362–366.
7. **Goff, S., P. Traktman, and D. Baltimore.** 1981. Isolation and properties of Moloney murine leukemia virus mutants: use of a rapid assay for release of virion reverse transcriptase. J. Virol. **38**:239–248.
8. **Grandgenett, D., T. Quinn, P. J. Hippenmeyer, and S. Oroszlan.** 1985. Structural characterization of the avian retrovirus reverse transcriptase and endonuclease domains. J. Biol. Chem. **260**: 8243–8249.
9. **Green, M. R.** 1986. Pre-mRNA splicing. Annu. Rev. Genet. **20**:671–708.
10. **Hirt, B.** 1967. Selective extraction of polyoma DNA from infected mouse cell cultures. J. Mol. Biol. **26**:365–369.
11. **Hwang, L.-H. S., J. Park, and E. Gilboa.** 1984. Role of intron-contained sequences in formation of Moloney murine leukemia virus *env* mRNA. Mol. Cell. Biol. **4**:2289–2297.
12. **Inoue, J.-I., M. Yoshida, and M. Seiki.** 1987. Transcriptional ($p40^x$) and post-transcriptional ($p27^{x\text{-}III}$) regulators are required for the expression and replication of human T-cell leukemia virus type I genes. Proc. Natl. Acad. Sci. USA **84**:3653–3657.
13. **Katz, R. A., and A. M. Skalka.** 1988. A C-terminal domain in the avian sarcoma-leukosis virus *pol* gene product is not essential for viral replication. J. Virol. **62**:528–533.
14. **Katz, R. A., R. W. Terry, and A. M. Skalka.** 1986. A conserved *cis*-acting sequence in the 5′ leader of avian sarcoma virus RNA is required for packaging. J. Virol. **59**:163–167.
15. **Keller, E. B., and W. A. Noon.** 1984. Intron splicing: a conserved internal signal in introns of animal pre-mRNAs. Proc. Natl. Acad. Sci. USA **81**:7417–7420.
16. **Konarska, M. M., and P. A. Sharp.** 1986. Electrophoretic separation of complexes involved in the splicing of precursors to mRNAs. Cell **46**:845–855.
17. **Konarska, M. M., and P. A. Sharp.** 1987. Interaction between small nuclear ribonucleoprotein particles in formation of spliceosomes. Cell **49**:763–774.

18. **Kopchick, J. J., and D. W. Stacey.** 1984. Differences in intracellular DNA ligation after microinjection and transfection. Mol. Cell. Biol. **4**:240–246.
19. **Lomedico, P. T.** 1982. Use of recombinant DNA technology to program eukaryotic cells to synthesize rat proinsulin: a rapid expression assay for cloned genes. Proc. Natl. Acad. Sci. USA **79**:5798–5802.
20. **Maniatis, T., E. F. Fritsch, and J. Sambrook.** 1982. Molecular cloning: a laboratory manual. Cold Spring Harbor Laboratory, Cold Spring Harbor, N.Y.
21. **Maniatis, T., and R. Reed.** 1987. The role of small nuclear ribonucleoprotein particles in pre-mRNA splicing. Nature (London) **325**:673–678.
22. **Maxam, A. M., and W. Gilbert.** 1980. Sequencing end-labeled DNA with base-specific chemical cleavages. Methods Enzymol. **65**:499–560.
23. **Miller, C. K., and H. M. Temin.** 1986. Insertion of several different DNAs in reticuloendotheliosis virus strain T suppresses transformation by reducing the amount of subgenomic mRNA. J. Virol. **58**:75–80.
24. **Mount, S. M.** 1982. A catalogue of splice junction sequences. Nucleic Acids Res. **10**:459–472.
25. **Nash, M. A., B. L. Brizzard, J. L. Wong, and E. C. Murphy, Jr.** 1985. Murine sarcoma virus ts110 RNA transcripts: origin from a single proviral DNA and sequence of the *gag-mos* junctions in both the precursor and spliced viral RNAs. J. Virol. **53**:624–633.
26. **Padgett, R. A., P. J. Grabowski, M. M. Konarska, S. Seiler, and P. A. Sharp.** 1986. Splicing of messenger RNA precursors. Annu. Rev. Biochem. **55**:1119–1150.
27. **Parker, R., P. G. Siliciano, and C. Guthrie.** 1987. Recognition of the TACTAAC box during mRNA splicing in yeast involves base pairing to the U2-like snRNA. Cell **49**:229–239.
28. **Schwartz, D. B., R. Tizard, and W. Gilbert.** 1983. Nucleotide sequence of Rous sarcoma virus. Cell **32**:853–869.
29. **Sharp, P. A.** 1987. Splicing of messenger RNA precursors. Science **235**:766–771.
30. **Solnick, D.** 1985. Alternative splicing caused by RNA secondary structure. Cell **43**:667–676.
31. **Stoltzfus, C. M., S. K. Lorenzen, and S. L. Berberich.** 1987. Noncoding region between the *env* and *src* genes of Rous sarcoma virus influences splicing efficiency at the *src* gene 3′ splice site. J. Virol. **61**:177–184.
32. **Weiss, R., N. Teich, H. Varmus, and J. Coffin (ed.).** 1984. Molecular biology of tumor viruses: RNA tumor viruses, 2nd ed. Cold Spring Harbor Laboratory, Cold Spring Harbor, N.Y.
33. **Wills, J. W., J. M. Hardwick, K. Shaw, and E. Hunter.** 1983. Alterations in the transport and processing of Rous sarcoma virus envelope glycoproteins mutated in the signal and anchor regions. J. Cell. Biochem. **23**:81–94.